MOUNTAIN-PLAINS CONSORTIUM

MPC 15-296 | J.W. van de Lindt and N. Nazari

Seismic Risk Assessment for
the I-25/I-70 Corridor
in the Mountain Plains
Region of the U.S.

Seismic Risk Assessment for the I-25/I-70 Corridor in the Mountain Plains Region of the U.S.

Prepared by

John W. van de Lindt
Negar Nazari

Colorado State University
Fort Collins

December 2015

Disclaimer

The contents of this report reflect the work of the authors, who are responsible for the facts and the accuracy of the information presented. This document is disseminated under the sponsorship of the Mountain-Plains Consortium in the interest of information exchange. The U.S. Government assumes no liability for the contents or use thereof.

Additionally, this report is the result of a very preliminary study with limited budget and thus the fragilities were approximated from existing fragility functions available as part of MAEViz/Ergo, software originally developed as part of the Mid-America Earthquake (MAE) Center.

ABSTRACT

When one thinks of earthquakes the Mountain Plains Region does not come to mind first; rather, the West Coast, South America, Japan, and, most recently, Italy and Nepal can easily be pictured. According to the U.S. Geological Survey (USGS) the largest earthquake on record for Colorado occurred in 1882: "The earthquake of November 7, 1882, the first ever to cause damage at Denver, probably centered in the Front Range near Rocky Mountain National Park, and is the largest historical earthquake in the state. The magnitude was estimated to be about 6.2 on the Richter scale. In Boulder County the walls of the depot cracked, and plaster fell from walls at the university at Boulder. The quake was felt as far away as Salina, Kansas and Salt Lake City, Utah.

Seismic hazard assessment in Colorado has demonstrated there is the potential for another event of this magnitude. Most structures in Colorado are designed with a focus on wind, which puts them at significant risk if an earthquake of M6 or greater were to occur, primarily because of a lack of seismic detailing which enables a structure to dissipate the energy input from load reversals. The seismic hazard situation in Colorado aligns with that of other parts of the United States and has been termed low-occurrence high-consequence. This hazard situation has created a challenge in terms of public perception, i.e. there is a perceived lack of need to consider this type of hazard.

According to the 2005 Regional Transportation Plan for the Intermountain Transportation Planning Region (2007), up to 38,000 vehicles travel I-70 each day and that traffic count is likely much higher now (2015). Consider what would happen if this traffic corridor was disrupted for some period of time, and perhaps if I-25, which intersects I-70, was also disrupted because of one or more bridge or overpass failures. This project examined a range of scenario events to gain a better understanding of the potential level of traffic disruption that might occur at the intersection of two main arterial freeways, namely Interstates 25 and 70.

TABLE OF CONTENTS

LIST OF FIGURES

LIST OF TABLES

1. INTRODUCTION AND SITE INFORMATION

Interstates 25 and 70 (I-25 and I-70) are major interstates that facilitate transportation from north to south and east to west in the United States, respectively, with average daily traffic of about 150,000 to 200,000. This highlights the need for continued functionality of these two interstates following a moderate earthquake. To perform an evaluation, the intersection of I-25 and I-70 was examined using existing fragility functions for typical bridges designed in non- or very moderate seismic regions of the United States. These fragilities were combined with expected mean accelerations from an assessment of site-to-source distance for several well-known faults that were thought to most likely to rupture. Figure 1.1 presents the location of the intersection and the overpasses. Figure 1.2 presents the street view of the intersection and the overpasses. This report evaluates the likely functionality of these interstates after an earthquake using the spectral acceleration and fragility curves mentioned above.
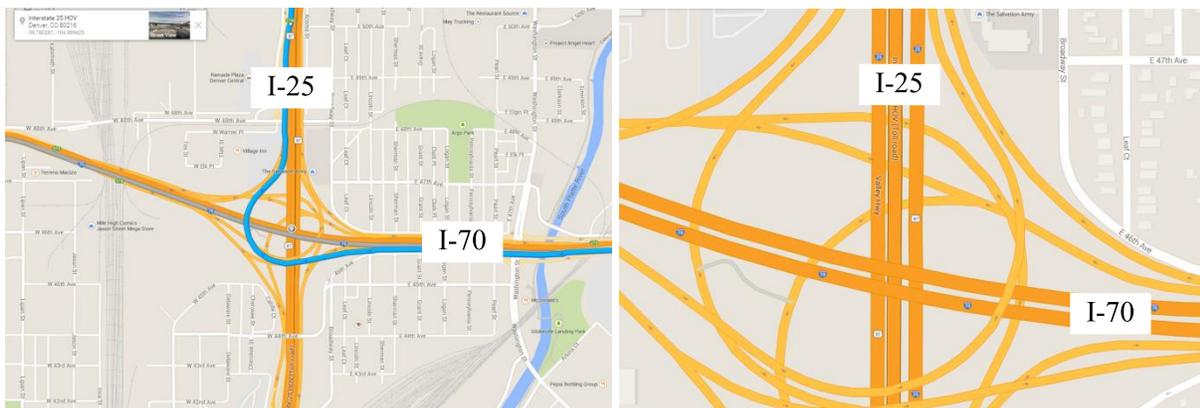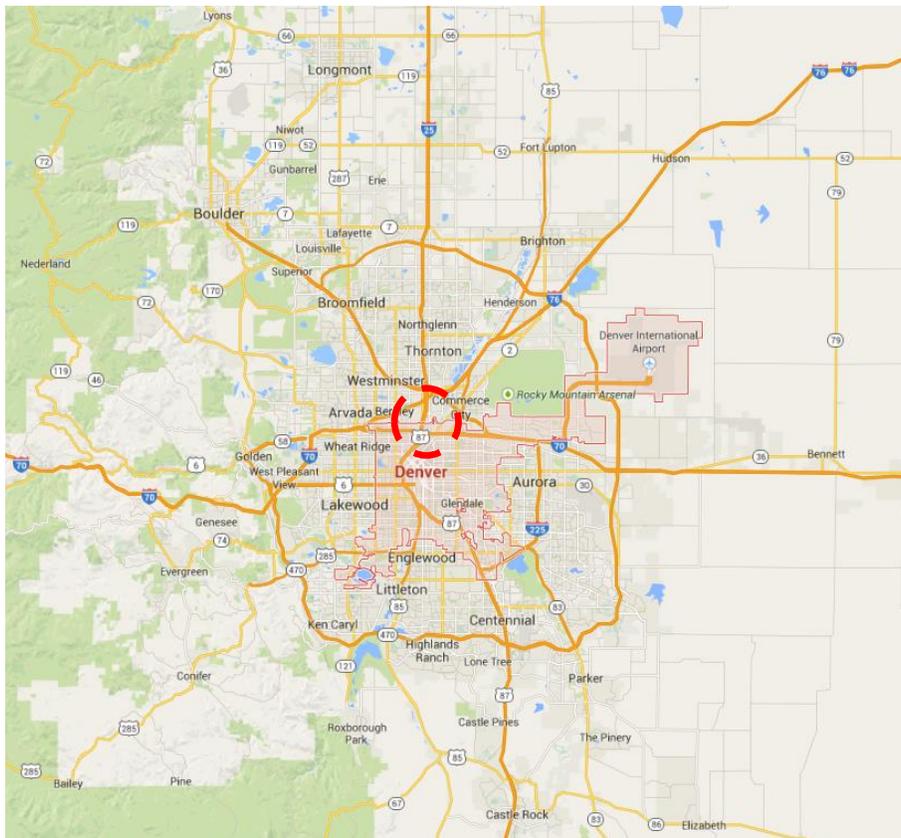
Figure 1.1 Location of the intersection of I-25 and I-70.

Figure 1.2 Location of the intersection of I-25 and I-70 (Google map©).

2. NEXT GENERATION ATTENUATION RELATIONSHIP

Also of key interest is assessing the likely spectral acceleration at the site of interest (Intersection of I-25 and I-70) from several likely fault locations in Colorado. Empirical ground-motion models for the rotation-independent average horizontal component from shallow crustal earthquakes have been derived using the PEER NGA database. The model is applicable to magnitudes 5-8.5, distances 0-200 km, and spectral periods of 0-10 sec. In place of generic site categories (soil and rock), the site is parameterized by average shear-wave velocity in the top 30 m (V_S30) and the depth to engineering rock (depth to V_S=1000 m/s). In addition to magnitude and style-of-faulting, the source term is also dependent on the depth to top-of-rupture: for the same magnitude and rupture distance, buried ruptures lead to larger short-period ground motions than surface ruptures. The hanging-wall effect is included with an improved model that varies smoothly as a function of the source properties (M, dip, depth), and the site location. The standard deviation is magnitude dependent with smaller magnitudes leading to larger standard deviations. The short-period standard deviation model for soil sites also is distant-dependent because of non-linear site response, with smaller standard deviations at short distances.
In previous ground-motion models, the range of applicability of the empirical ground motion models was based on the range covered by the available empirical data set. However, in hazard studies, the ground motion must be computed for all relevant earthquakes, so the limits on the range of applicability were often ignored. To address this issue, the Next Generation Attenuation (NGA) project required the developers of the models to extrapolate their models such that they are applicable to all crustal earthquakes relevant for seismic hazard analyses in California: M5 M8.5 for strike-slip, M5-M8.0 for dip-slip, distance 0-200 km, and spectral periods up to 10 seconds.

A recurring comment on the NGA project is that the empirical data is not adequate to constrain the ground motion over the entire specified range. The concept behind the NGA project is that the developers are better suited than the hazard analyst to extrapolate their models for application outside the range well constrained by the empirical data. To support the developers in this extrapolation, the NGA project used three classes of analytical models to provide the developers with constraints on the ground-motion scaling outside the range well constrained by the empirical data. These analytical models included hard-rock ground motions based on 1-D finite-fault kinematic source models for M6.5 to M8.25 (Collins et al., 2006), 3-D basin response simulations for sites in southern California (Day et al., 2006), and equivalent-linear site response simulations (Walling et al., 2008). The development of the NGA models is not simple curve fitting, but rather, it is model building that uses seismological and geotechnical information, in addition to the empirical ground-motion data, to develop the models. The NGA models are intended to begin the transition from simple empirical models to full numerical simulations for specific source-site geometries.

3.   PRODUCING SPECTRAL ACCELERATION

To produce the spectral acceleration induced by each fault at the I25/I70 intersection, the parameters of the Southern Sawatch Fault, the Northern Sangre de Cristo Fault, and the Cheraw Fault were used to produce the spectral accelerations induced by earthquakes with magnitudes in the range of M5.8 to M7.0. Then, the following steps were taken to produce the spectral accelerations:

Step 1. Identify the longitude and latitude of intersection of I-25 and I-70 as the site (Latitude: 39.780287, Longitude -104.989425).
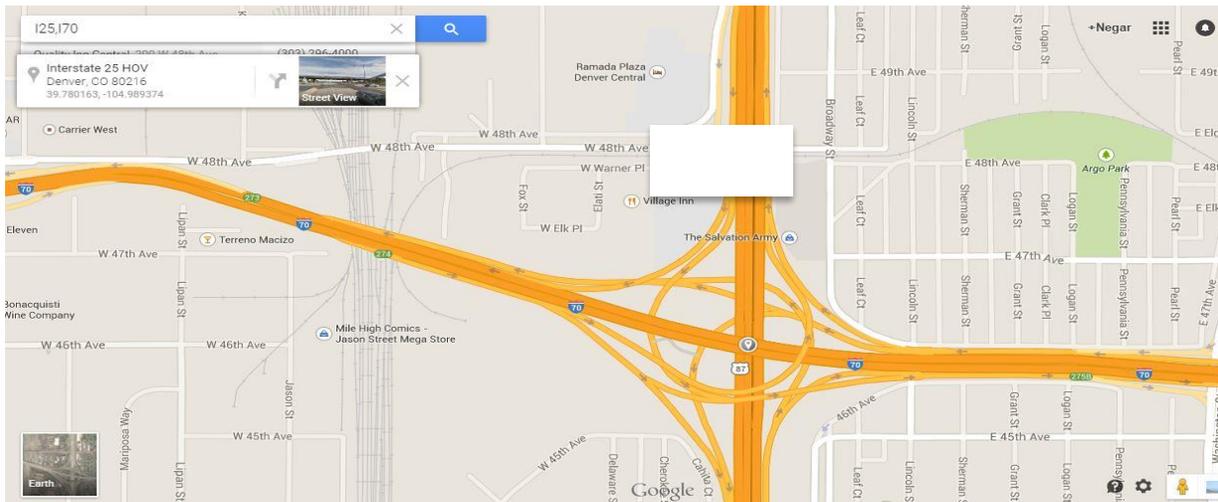
Figure 3.1 Coordinates of I-25 and I-70 intersection.

Step 2. Identify faults in Colorado in a radius R=300 km using information from the 2008 National Seismic Hazard Maps and the USGS Geo Hazard metadata (http://geohazards.usgs.gov/cfusion/hazfaults_search/hf_search_main.cfm). Based on the site-to-source distance calculated above and other parameters from the NGA 2008 (Abrahamson and Silva), generate the spectral acceleration values. All three fault types are normal as shown in Figure 3.2 and fault details are presented in Figures 3.3 through 3.5.

Output	Distance in Kilometers	Name	St Fault parallel slip rate	Preferred Dip (degrees)	Dip Dir	Slip Sense	Rupture Top (km)	Rupture Bottom (km)	Length (km)
✓	141.39	Southern Sawatch fault	CO0.08	50	E	normal	0	15	45
✓	176.81	Northern Sangre de Cristo fault	CO0.23	50	W	normal	0	15	185
✓	213.86	Cheraw fault	CO0.17	60	NW	normal	0	15	45
✓	292.34	Southern Sangre de Cristo fault	NM0.17	50	W	normal	0	15	103

Figure 3.2 Source Parameters for each fault - Data from 2008 National Seismic Hazard Maps

Fault Name	State
Northern Sangre de Cristo fault	Colorado

MODEL VALUES

Slip rate (vertical or horizontal in mm/yr)	0.18
Probability of activity	1
Minimum magnitude	6.5
Maximum magnitude	7.5

FAULT GEOMETRY

Dip (degrees)	60/40/50
Dip direction	W
Sense of slip	normal
Rupture top (km)	0
Rupture bottom (km)	15
Rake (degrees)	-90
Length (km)	185

Assigned Dip	Fault Parallel Slip Rate	Width	Characteristic Magnitude	Characteristic Rate	GR a-value	GR b-value	Weight
40	0.28	23.3	7.50		1.662	0.8	0.2
50	0.23	19.6	7.50		1.510	0.8	0.6
60	0.21	17.3	7.50		1.403	0.8	0.2

Figure 3.3 Northern Sangre de Cristo Fault Parameters - Data from 2008 National Seismic Hazard Maps

Fault Name	State
Southern Sawatch fault	Colorado

MODEL VALUES

Slip rate (vertical or horizontal in mm/yr)	0.062
Probability of activity	1
Minimum magnitude	6.5
Maximum magnitude	6.99

FAULT GEOMETRY

Dip (degrees)	50/40/60
Dip direction	E
Sense of slip	normal
Rupture top (km)	0
Rupture bottom (km)	15
Rake (degrees)	-90
Length (km)	45

Assigned Dip	Fault Parallel Slip Rate	Width	Characteristic Magnitude	Characteristic Rate	GR a-value	GR b-value	Weight
40	0.10	23.3	6.99	8.80e-05	1.095	0.8	0.2
50	0.08	19.6	6.99	6.19e-05	0.943	0.8	0.6
60	0.07	17.3	6.99	4.85e-05	0.836	0.8	0.2

Figure 3.4 Southern Sawatch Fault Parameters - Data from 2008 National Seismic Hazard Maps

Fault Name	State
Cheraw fault	Colorado

MODEL VALUES	
Slip rate (vertical or horizontal in mm/yr)	0.15
Probability of activity	1
Minimum magnitude	6.5
Maximum magnitude	7

FAULT GEOMETRY	
Dip (degrees)	60
Dip direction	NW
Sense of slip	normal
Rupture top (km)	0
Rupture bottom (km)	15
Rake (degrees)	-90
Length (km)	45

Figure 3.5 Cheraw Fault Parameters – Data from 2008 National Seismic Hazard Maps

Figures 3.6, 3.7 and 3.8 present the spectral acceleration for a 5% damped single-degree-of-freedom system as a function of fundamental period of T_n produced by the aforementioned technique for each fault. It can be seen that the spectral accelerations increase as the magnitude of earthquakes increases, as should be expected. Table 3.1 presents the spectral acceleration at T_n = 0.2 s for earthquakes with magnitude ranging from M5.6 to M7.0 for all three faults. Overpass columns tend to be quite stiff and have an estimated natural period of vibration of T_n = 0.2 seconds.
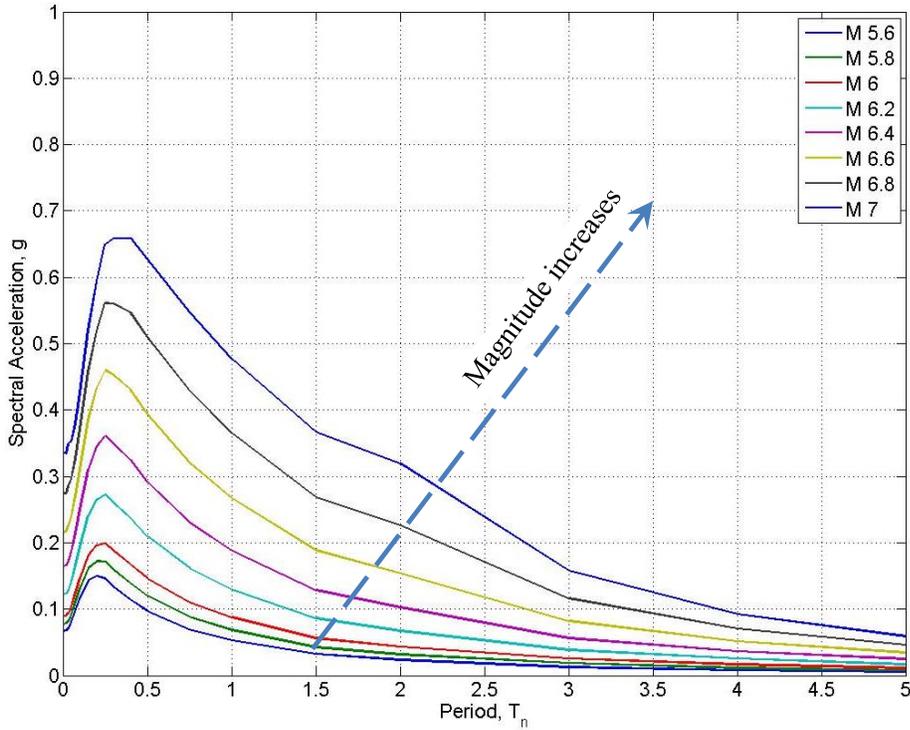
Figure 3.6 Spectral acceleration for different earthquake magnitudes induced by Southern Sawatch Fault.
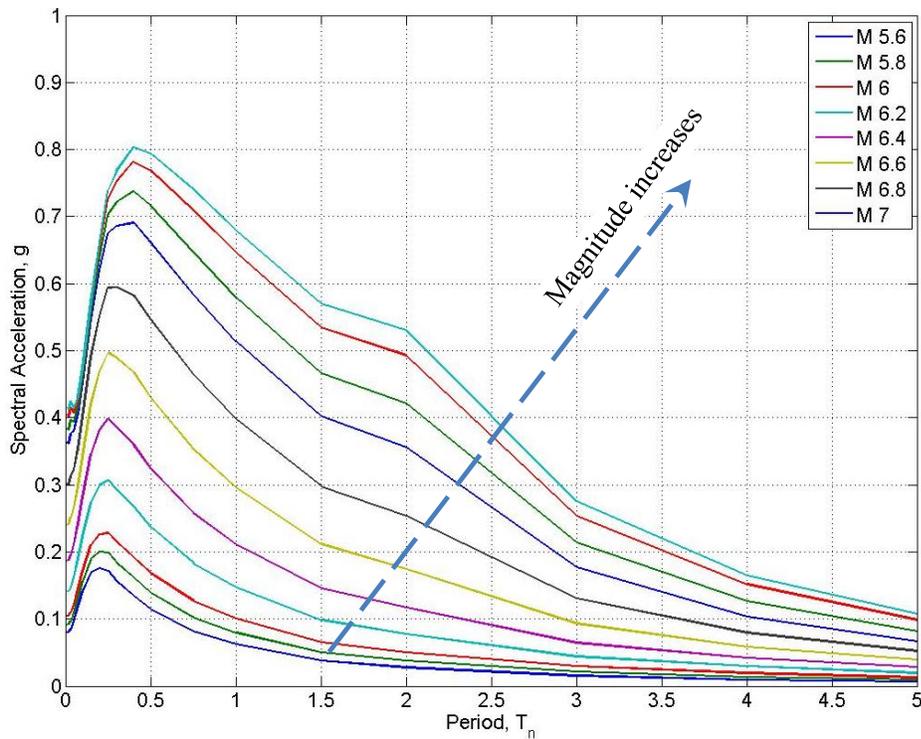
Figure 3.7 Spectral acceleration for different earthquake magnitudes induced by Northern Sangre de Cristo Fault.
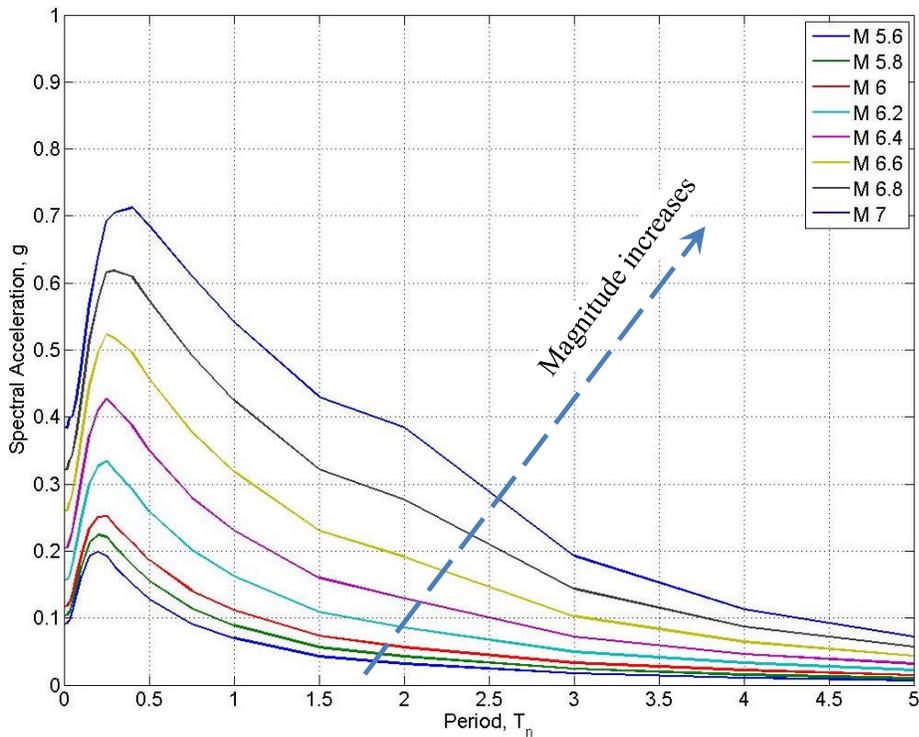
Figure 3.8 Spectral acceleration for different earthquake magnitudes induced
by Cheraw Fault.

Table 3.1 Spectral acceleration induced by each fault for different earthquake magnitudes

| Magnitude | Spectral accelerations, g | | |
	Southern Sawatch Fault	Northern Sangre de Cristo Fault	Cheraw Fault
5.6	0.15	0.18	0.20
5.8	0.17	0.20	0.22
6	0.20	0.23	0.25
6.2	0.26	0.30	0.33
6.4	0.35	0.38	0.41
6.6	0.43	0.47	0.50
6.8	0.52	0.55	0.57
7	0.59	0.62	0.64

4. FRAGILITY CURVES AND EVALUATION

To estimate the functionality of the over pass and the bridges, the fragility curves produced by Hwang et al, 2001 were used in this report. Four different damage states were introduced by Hwang et al., namely: (1) slight damage, (2) moderate damage, (3) extensive damage, and (4) complete damage. The spectral acceleration corresponding to $T_n= 0.2$ sec were extracted from the spectral acceleration plots. The $T_n = 0.2$ sec was used based on the research conducted by Wilson et al, 2013. Figures 4.1, 4.2 and 4.3 present the fragility curves for the four different damage states with the spectral acceleration induced by earthquakes with different magnitudes (i.e., vertical dashed lines). It can be seen that the probability of exceeding a damage state increases as the magnitude of the earthquakes increases. The probability of exceeding damage states for earthquakes with different magnitudes generated by the Southern Sawatch Fault, the Northern Sangre de Cristo Fault, and the Cheraw Fault are presented in Tables 4.1, 4.2 and 4.3, respectively. For example, the probability of exceeding the moderate damage state for an earthquake with a magnitude of M7.0 generated by the Southern Sawatch Fault, Northern Sangre de Cristo Fault, and Cheraw Fault are 72%, 76%, and 78%, respectively.
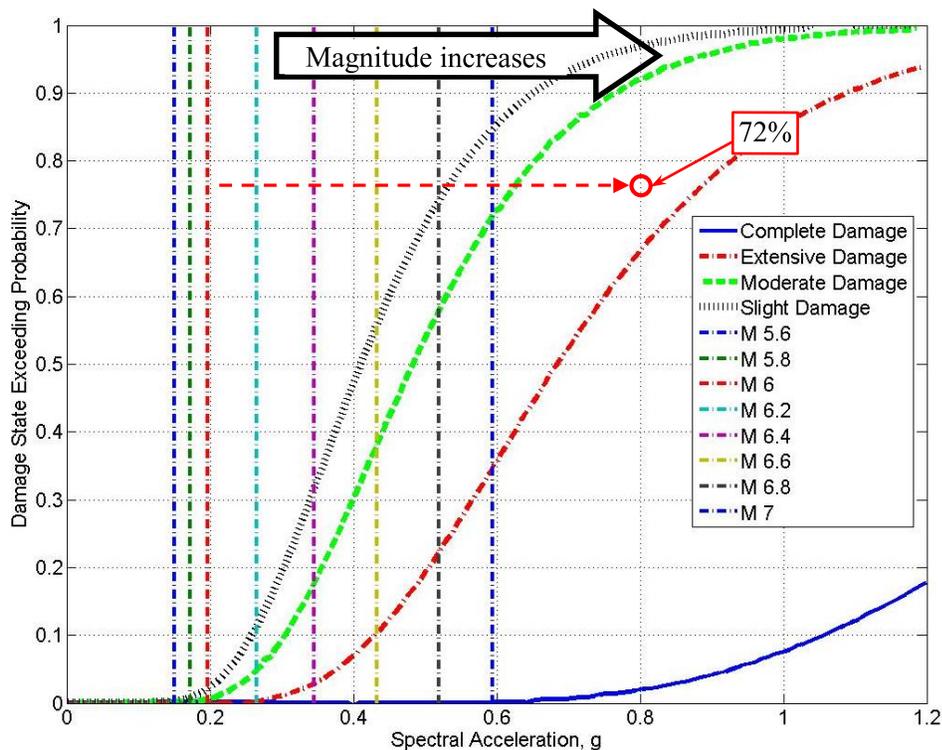
Figure 4.1 Fragility curves and spectral acceleration corresponding to $T_n = 0.2$ sec induced by Southern Sawatch Fault

Table 4.1 Probability of exceeding damage states at different magnitude earthquakes induced by Southern Sawatch Fault

Level of Damage	Damage state exceeding probability corresponding to earthquake magnitude (%)							
	M5.6	M5.8	M6.0	M6.2	M6.4	M6.6	M6.8	M7.0
Slight Damage	1	2	3	11	32	56	74	85
Moderate Damage	1	1	2	5	17	39	58	72
Extensive Damage	1	1	1	1	3	11	23	35
Complete Damage	1	1	1	1	1	1	1	1
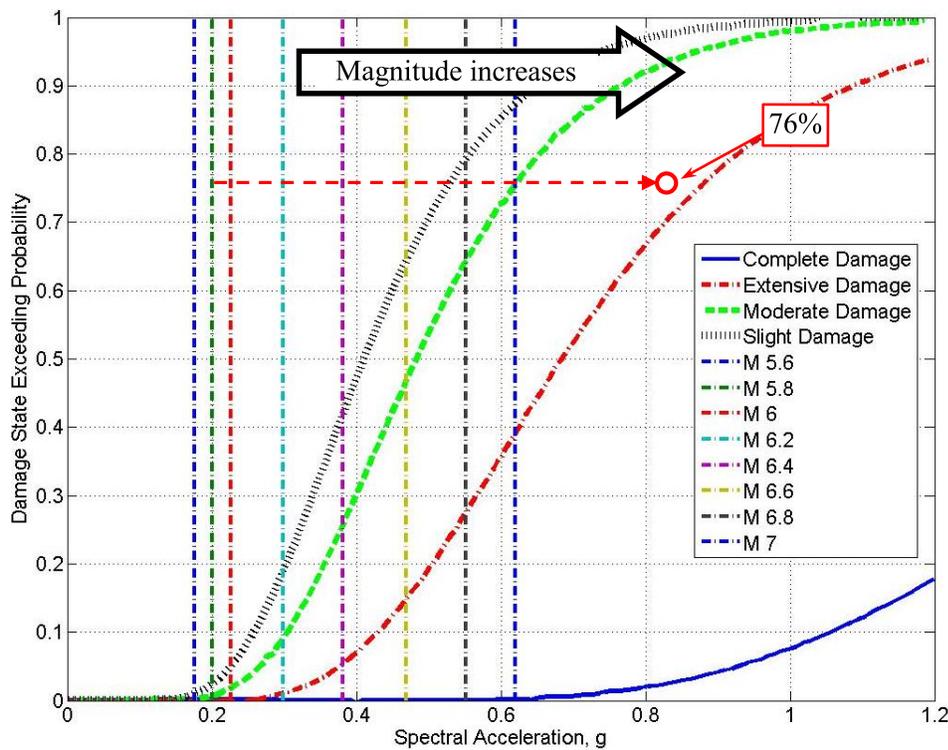
Figure 4.2 Fragility curves and spectral acceleration corresponding to $T_n = 0.2$ sec induced by Northern Sangre de Cristo Fault

Table 4.2 Probability of exceeding damage states at different magnitude earthquakes induced by Northern Sangre de Cristo Fault

| Level of Damage	Damage state exceeding probability corresponding to earthquake magnitude (%)							
	M5.6	M5.8	M6.0	M6.2	M6.4	M6.6	M6.8	M7.0
Slight Damage	2	3	5	19	42	64	79	88
Moderate Damage	1	2	3	9	26	48	64	76
Extensive Damage	1	1	1	2	5	15	28	39
Complete Damage	1	1	1	1	1	1	1	1.5
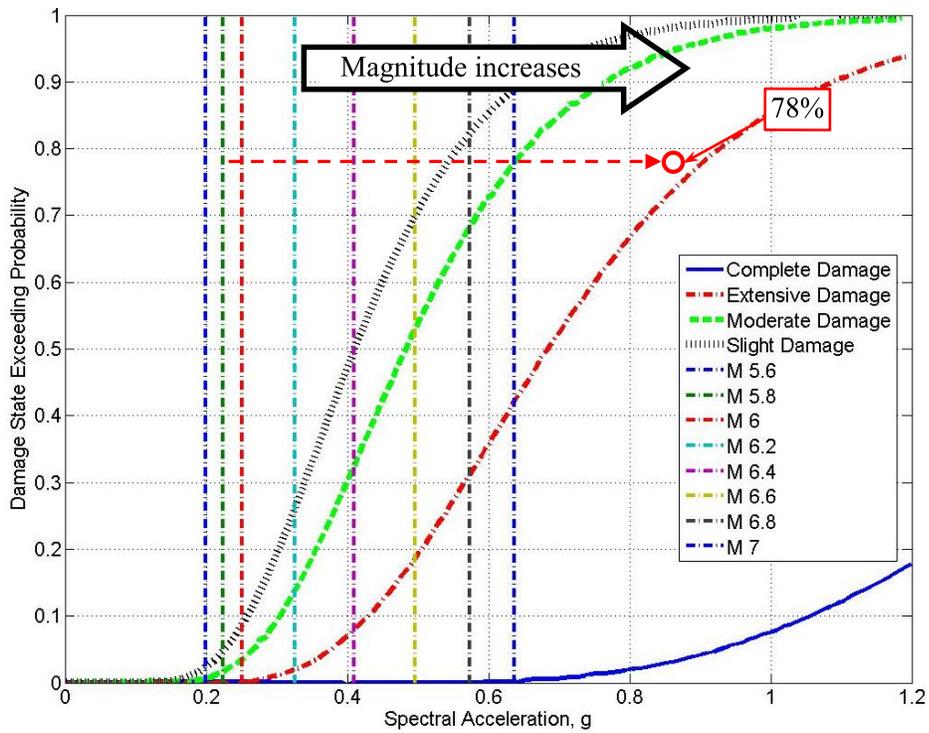
Figure 4.3 Fragility curves and spectral acceleration corresponding to T_n = 0.2 sec induced by Cheraw Fault

Table 4.3 Probability of exceeding damage states at different magnitude earthquakes induced by Cheraw Fault

Level of Damage	Damage state exceeding probability corresponding to earthquake magnitude (%)							
	M5.6	M5.8	M6.0	M6.2	M6.4	M6.6	M6.8	M7.0
Slight Damage	3	4	9	26	50	70	82	89
Moderate Damage	2	2.5	4	14	32	53	69	78
Extensive Damage	1	1	1	2.5	18	19	31	42
Complete Damage	1	1	1	1	1	1	1	1.5

5. APPROXIMATE EFFECT OF DAMAGE ON ANNUAL AVERAGE DAILY TRAFFIC (AADT)

To investigate the effect of damage caused by an earthquake, the effect of different levels of damage on the annual average daily traffic (AADT) of each interstate was investigated. Based on data recorded by Colorado Department of Transportation (CDOT) in 2013, the AADT of I-25 and I-70 were 202,000 and 153,000, respectively. In this study, it is assumed that each damage level decreases the AADT by 25%. For example, if the I-70 overpass damage is classified as the slightly damaged level, then the AADT of I-70 may approximately decrease from 153,000 to 114,750. Table 5.1 presents the AADT for both I-25 and I-70 for different level of damage.
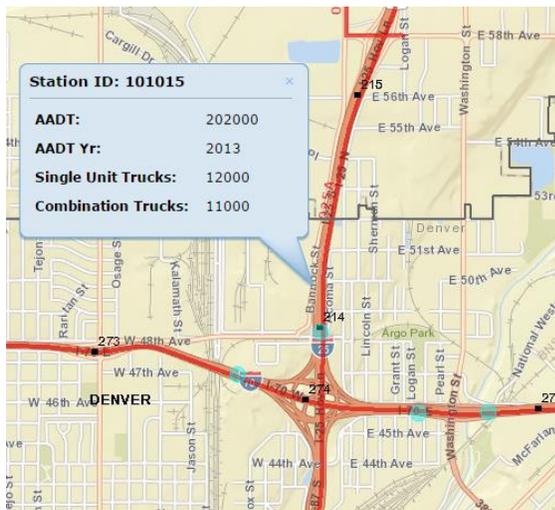
Figure 5.1 AADT of I-25 recorded in 2013
Data from Colorado Department of Transportation
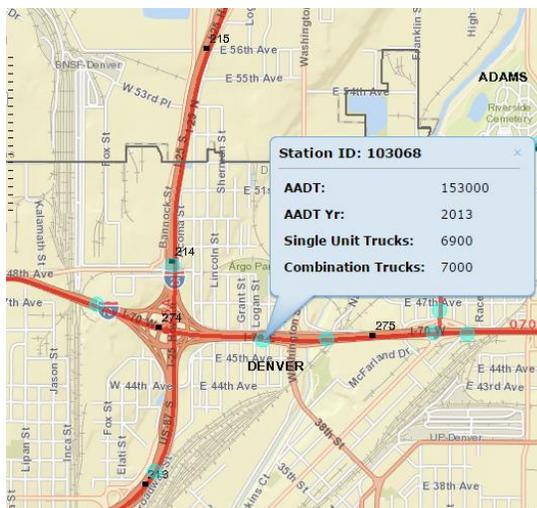
Figure 5.2 AADT of I-70 recorded in 2013
Data from Colorado Department of Transportation

Table 5.1 AADT of I-25 and I-70 corresponding to different level of damage

Level of Damage	Percentage of AADT passed	Reduced AADT I-25	Reduced AADT I-70
No Damage	100	202000	153000
Slight Damage	75	151500	114750
Moderate Damage	50	101000	76500
Extensive Damage	25	50500	38250
Complete Damage	0	0	0

6. DISCUSSION AND INTERPRETATION OF DATA

If one was to assume a scenario of having a magnitude M7.0 earthquake caused by a rupture on the Southern Sawatch fault, according to Table 1, such a magnitude earthquake can produce a spectral acceleration of 0.59g. This would correspond to probability of exceeding slight damage, moderate damage, extensive damage, and complete damage of 85%, 72%, 35%, and 1%, respectively. This means that, for example, the probability of having a 25% decrease in AADT of I-25 and I-70 is about 85%, in the event of an earthquake with the magnitude of M7.0 caused by a rupture at Southern Sawatch fault. Obviously, these are approximate and based on a number of traffic scenarios which are likely conservative. It also is likely that traffic would be disrupted even more severely because of the nonlinear relationship between any type of traffic disruption and the flow of traffic.

7. SUMMARY AND CONCLUSIONS

In this summary report, the approximate damage that would result to overpasses at the intersection of two main Colorado arterial roadways, I-25 and I-70, was identified using a combination of a well-known attenuation equation and damage fragility curves for lightly reinforced overpasses. The level of damage and resulting traffic disruption varied as a function of earthquake magnitude as could be expected. From this study it is clear that, for an earthquake greater than M6.0, there would be disruption to traffic, and for an earthquake of M7.0, this disruption would be quite significant to traffic flow and for freight traveling both east-west and north-south.

REFERENCES

Abrahamson, N. A., and W. J. Silva. (2008). "Summary of the Abrahamson & Silva NGA ground-motion relations." *Earthquake Spectra* 24: 67–97.

Hwang, H., Liu, J. B., and Chiu, Y. (2001). "Seismic Fragility Analysis of Highway Bridges", Center for Earthquake Research and Information, The University of Memphis.

Collins, N., Graves, R., and Somerville, P. (2006) Revised analysis of 1-D rock simulations for the NGA-E project, Final report prepared for the Pacific Earthquake Engineering Research Center.

Colorado Department of Transportation, Traffic Data Explorer, http://dtdapps.coloradodot.info/otis/trafficdata#ui/1/0/0/criteria/20000//true/true/

Day, S. M., Bielak, J., Dreger, D., Graves, R., Larsen, S., Olsen, K., and Pitarka, A. (2005). 3D ground motion simulations in basins, Final report prepared for the Pacific Earthquake Engineering Research Center, Project 1A03.

Walling, M., Silva, W. J., and Abrahamson, N. A. 2008. "Nonlinear site amplification factors for constraining the NGA models." *Earthquake Spectra* 24: 243–255.

Wilson, T., Mahmoud, H., Chen, S. (2013). "Seismic performance of skewed and curved reinforced concrete bridges in mountainous states," *Engineering Structures*, 70 (2014): 158–167.

USGS Geo Hazard metadata, http://geohazards.usgs.gov/cfusion/hazfaults_search/hf_search_main.cfm